Research Article | Vol. 26, No. 6 | 19 Mar 2018 | OPTICS EXPRESS A275
Optics EXPRESS

Mesoscale trumps nanoscale: metallic mesoscale contact morphology for improved light trapping, optical absorption and grid conductance in silicon solar cells

REBECCA SAIVE[1,2] AND HARRY A. ATWATER[1,3]

[1]*Californina Institute of Technology, Pasadena, CA 91106, USA*
[2]*r.saive@utwente.nl*
[3]*haa@caltech.edu*

Abstract: We report on a computational study exploring the design of mesoscale metallic front contacts for solar cells. We investigated silver contact structures with circle, triangle and square cross-sections for various length scales and surface coverages. We found that for 'nanoscale' contacts with widths between 10 nm and 1000 nm, resonant coupling actually impairs light absorption in the semiconductor. Conversely, for 'mesoscale' contact widths > 1000 nm, the light interaction is determined by the geometric shadowing. We find that mesoscale silver contacts with triangular cross-section outperform other nanostructure morphologies in reducing shadow losses and yield contact transparency of >99% percent with sheet resistance <0.2 Ω/sq. Surprisingly, very densely spaced mesoscale silver triangular cross-section contacts can enhance the absorption of thin silicon/silver structures by up to 15% at a front contact coverage of 83%, due to light trapping by the front contact. Such structures can also maintain up to 100% absorption within the silicon, at a front contact coverage of 50%, relative to the same structure without metal.

OCIS codes: (350.6050) Solar energy; (350.3950) Micro-optics; (350.4238) Nanophotonics and photonic crystals.

References and links

1. A. Blakers, "Shading losses of solar cell metal grids," J. Appl. Phys. **71**(10), 5237–5241 (1992).
2. M. Morales-Masis, S. De Wolf, R. Woods-Robinson, J. W. Ager, and C. Ballif, "Transparent Electrodes for Efficient Optoelectronics," Adv. Electron. Mater. **3**(5), 1600529 (2017).
3. J. S. Ward, A. Duda, D. J. Friedman, J. Geisz, W. McMahon, and M. Young, "High aspect ratio electrodeposited Ni/Au contacts for GaAs based III–V concentrator solar cells," Prog. Photovolt. Res. Appl. **23**(5), 646–653 (2015).
4. J. Lossen, D. Rudolph, L. J. Koduvelikulathu, R. Carvalho, M. P. Rossetto, O. Borsato, E. Bortoletto, and M. Galiazzo, "Double Printing nPERT Cells with Narrow Contact Layers," Energy Procedia **92**, 939–948 (2016).
5. M. F. Schumann, S. Wiesendanger, J. C. Goldschmidt, B. Bläsi, K. Bittkau, U. W. Paetzold, A. Sprafke, R. B. Wehrspohn, C. Rockstuhl, and M. Wegener, "Cloaked contact grids on solar cells by coordinate transformations: designs and prototypes," Optica **2**(10), 850–853 (2015).
6. P. G. Kik, "Catoptric electrodes: transparent metal electrodes using shaped surfaces," Opt. Lett. **39**(17), 5114–5117 (2014).
7. R. Saive, C. R. Bukowsky, S. Yalamanchili, M. Boccard, T. Saenz, A. M. Borsuk, Z. Holman, and H. A. Atwater, "Effectively transparent contacts (ETCs) for solar cells," in *IEEE* 43rd *Photovoltaic Specialists Conference (PVSC)* (2016), pp. 3612–3615.
8. R. Saive, A. M. Borsuk, H. S. Emmer, C. R. Bukowsky, J. V. Lloyd, S. Yalamanchili, and H. A. Atwater, "Effectively Transparent Front Contacts for Optoelectronic Devices," Adv. Opt. Mater **4**(10), 1470–1474 (2016).
9. R. Saive, M. Boccard, T. Saenz, S. Yalamanchili, C. R. Bukowsky, P. Jahelka, Z. J. Yu, J. Shi, Z. Holman, and H. A. Atwater, "Silicon heterojunction solar cells with effectively transparent front contacts," Sustain. Energy Fuels **1**(3), 593–598 (2017).
10. H. A. Atwater, R. Saive, A. M. Borsuk, H. Emmer, C. Bukowsky, and S. Yalamanchili, "Solar Cells and Methods of Manufacturing Solar Cells Incorporating Effectively Transparent 3D Contacts," (US Patent, 2016).
11. Z. Zhao, K. X. Wang, and S. Fan, "Analysis of an anti-reflecting nanowire transparent electrode for solar cells," J. Appl. Phys. **121**(11), 113109 (2017).
12. T. Gao and P. W. Leu, "The role of propagating modes in silver nanowire arrays for transparent electrodes," Opt. Express **21**(S3 Suppl 3), A419–A429 (2013).

#319240 https://doi.org/10.1364/OE.26.00A275
Journal © 2018 Received 2 Feb 2018; revised 21 Feb 2018; accepted 22 Feb 2018; published 6 Mar 2018

Optics EXPRESS

13. S. Xie, Z. Ouyang, N. Stokes, B. Jia, and M. Gu, "Enhancing the optical transmittance by using circular silver nanowire networks," J. Appl. Phys. **115**(19), 193102 (2014).
14. V. K. Narasimhan, T. M. Hymel, R. A. Lai, and Y. Cui, "Hybrid Metal-Semiconductor Nanostructure for Ultrahigh Optical Absorption and Low Electrical Resistance at Optoelectronic Interfaces," ACS Nano **9**(11), 10590–10597 (2015).
15. J. V. Deelen, A. Omar, and M. Barink, "Optical Design of Textured Thin-Film CIGS Solar Cells with Nearly-Invisible Nanowire Assisted Front Contacts," Materials (Basel) **10**(12), 392 (2017).
16. R. Saive, C. R. Bukowsky, and H. Atwater, "Three-dimensional nanoimprint lithography using two-photon lithography master samples," https://arXiv:1702.04012v1 (2017).
17. M. A. Green, "Self-consistent optical parameters of intrinsic silicon at 300K including temperature coefficients," Sol. Energy Mater. Sol. Cells **92**(11), 1305–1310 (2008).
18. J. van de Groep, P. Spinelli, and A. Polman, "Transparent Conducting Silver Nanowire Networks," Nano Lett. **12**(6), 3138–3144 (2012).
19. P.-C. Hsu, S. Wang, H. Wu, V. K. Narasimhan, D. Kong, H. Ryoung Lee, and Y. Cui, "Performance enhancement of metal nanowire transparent conducting electrodes by mesoscale metal wires," Nat. Commun. **4**, 2522 (2013).
20. M. Taguchi, A. Yano, S. Tohoda, K. Matsuyama, Y. Nakamura, T. Nishiwaki, K. Fujita, and E. Maruyama, "24.7% record efficiency HIT solar cell on thin silicon wafer," IEEE J. Photovolt. **4**(1), 96–99 (2014).
21. W. M. Haynes, CRC handbook of chemistry and physics (CRC press, 2014).
22. G. Reeves and H. Harrison, "Obtaining the specific contact resistance from transmission line model measurements," IEEE Electron Device Lett. **3**(5), 111–113 (1982).
23. S.-H. Park, N. Kharche, D. Basu, Z. Jiang, S. Nayak, C. Weber, G. Hegde, K. Haume, T. Kubis, and M. Povolotskyi, "Scaling effect on specific contact resistivity in nano-scale metal-semiconductor contacts," in 71st Annual IEEE Device Research Conference (2013), pp. 125–126.
24. S. Braun, G. Micard, and G. Hahn, "Solar cell improvement by using a multi busbar design as front electrode," Energy Procedia **27**, 227–233 (2012).

1. Introduction

Metallic contact grids are a crucial component of most semiconductor devices as they enable charge carrier transport, injection and extraction. High lateral conductivity as well as low contact resistance are important for efficient device performance. In optoelectronic devices such as photodiodes and solar cells, additional attention needs to be paid to the optical properties. Usually, high metal coverage comes at the price of reduced transmission of light into the semiconductor, and in turn reduced photocurrent. Nevertheless, in many cases it is inevitably necessary to cover some finite area fraction of the semiconductor with metal in order to achieve low electrical resistance. Traditionally, solar cells use a metal grid optimized for optical and electrical performance and composed of silver grid fingers several tens of micrometers wide that are connected to millimeter-wide busbars. These structures are significantly larger than the wavelengths of above-bandgap light in the solar spectrum and therefore, their interaction with light can typically be described by ray optical models as shown in Fig. 1(c). The reduction in semiconductor absorption is proportional to the areal coverage of these grid fingers, and can be slightly lower in solar modules relative to bare cells due to total internal reflection within the module glass and encapsulation [1]. Great effort has been devoted to overcoming these metal shadowing losses by using transparent conductive oxides (TCOs) [2], high aspect ratio metal contacts [3, 4], cloaked contacts [5] and structures with beneficial geometries such as nanowire networks [6–13]. In some instances, a high metal coverage can actually be beneficial beyond improved electrical conductivity- e.g. large metal surface area can improve light trapping in thin absorbers, as shown in this paper and the performance of photocatalysts can be enhanced by increased metal fraction. In solar cells, the costly and parasitically absorbing TCOs often required in cells with low sheet conductance can be omitted if the grid finger sheet resistance can be made sufficiently low. It has been shown that the tradeoff between coverage and absorption can be partially overcome by funneling the light using nanotextured absorber materials that necessitate patterning of the absorber layer [14, 15]. However, in many high efficiency photovoltaics, the semiconductor surface cannot be structured or patterned to achieve this effect, because of the detrimental effect of patterning-induced damage on device electronic performance. Here, we present a computational study of the transmission, reflection and absorption of broadband light in

Optics EXPRESS

semiconductors covered with metallic structures with different shapes, different widths *w,* and different metal coverages. We investigated circular, triangular and square cross-section grid finger shapes in the nanoscale (w<<λ), mesoscale (w ≥ λ) and macroscale regimes (w>>λ) [Fig. 1]. We found the highest transmission for mesoscale triangular cross-section grid fingers with width >2.5 μm and width to height aspect ratio 1:3. These mesoscale grid fingers offer the advantage of essentially ray optical light interaction while still being densely spaced so that the use of TCOs can be omitted in e.g., silicon heterojunction solar cell applications. Furthermore, we demonstrate increased light absorption in thin silicon due to light trapping with densely spaced triangle silver structures.

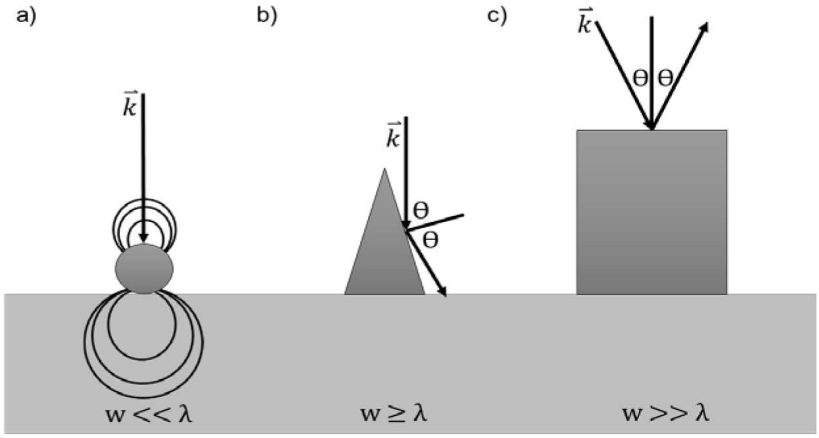

Fig. 1. Schematic of the interaction of light with wave vector and metal structures of width w in the a) nanoscale (w<<λ), b) mesoscale (w ≥ λ) and c) macroscale (w>>λ).

2. Metallic grids with different shapes, sizes and spacing

We performed computational optical simulations of free-standing silver structures in order to obtain information on the intrinsic properties of metallic structures with different shapes, sizes and spacing. Silver structures with circular, triangular and square cross-section were considered, the triangular cross-section featuring an aspect ratio of width:height = 1:3. Widths ranging across several length scales were considered: 10 nm, 50 nm, 100 nm, 250 nm, 500 nm 1000 nm, 2500 nm and 5000 nm. The coverage was varied between 5% and 63%, We used the software package DifractMOD by RSoft which performs rigorous coupled wave analysis (RCWA). Proper convergence was ensured by a harmonics study which resulted in the use of 100 harmonics. The index resolution was chosen to be one tenth of the structure height. Simulations were performed in two dimensions assuming an infinite length out of plane. A monochromatic plane wave was launched from the simulation cell top boundary and transmission to the rear boundary, reflection to the top boundary as well as absorption within the metal structures were computed. Triangular cross-section grid fingers were oriented with the triangular apex pointing towards the top boundary from which the light was incident. Wavelength dependent transmission of free-standing silver triangles, circles and squares with different widths is presented in Fig. 2(a)-2(c) for constant coverage of 10%. It can be seen that although shape and coverage are constant, the transmission strongly depends on the base width and on the shape. In particular the 50 nm, 100 nm and 250 nm structures experience strongly reduced transmission for specific wavelengths. Circle and square structures show sharper resonances as they feature less different radii along their height. Figure 2(e) and 2(f) show the reflection and absorption of free-standing silver triangles respectively. The reduced transmission is a result of the combination of several different effects. Absorption due to the

Optics EXPRESS

intrinsic material properties of silver plays the dominant role for light with wavelengths shorter than 400 nm, as can be seen in Fig. 2(f). Furthermore, the absorption is enhanced for nanostructures due to resonant interactions. The most significant loss in transmission results from reflection. For structures larger than 2.5 μm, the reflection is dominated by geometric optical scattering. In the nanoscale regime, resonant interactions depending on the width and periodicity of the grid dominate the reflection. The resonances become less pronounced for structures with wider base and completely disappear for width >2500 nm. In the case of circles and spheres the transmission approaches the uncovered area i.e. 90% of the incoming light. In contrast, the triangle transmission reaches almost 1, incoming light is reflected and redirected towards the transmission plane [8]. An aspect ratio of 1:3 for the triangular cross-section silver fingers was chosen for several reasons, considering the optical and electrical performance as well as practical limitations. A high aspect ratio leads to a low electrical resistance due to the large cross-section for current conduction. Furthermore, with high aspect ratio, incident light hits the structure under an oblique angle. The reflection of silver increases under more oblique angles and therefore, a high aspect ratio of the triangle cross-section also improves the optical properties. For practical reasons the aspect ratio is limited. We have demonstrated fabrication of triangular cross-section silver lines with high fidelity with a cross-section of up to 1:3 [7–9, 16] and therefore, chose 1:3 as the aspect ratio for this study.

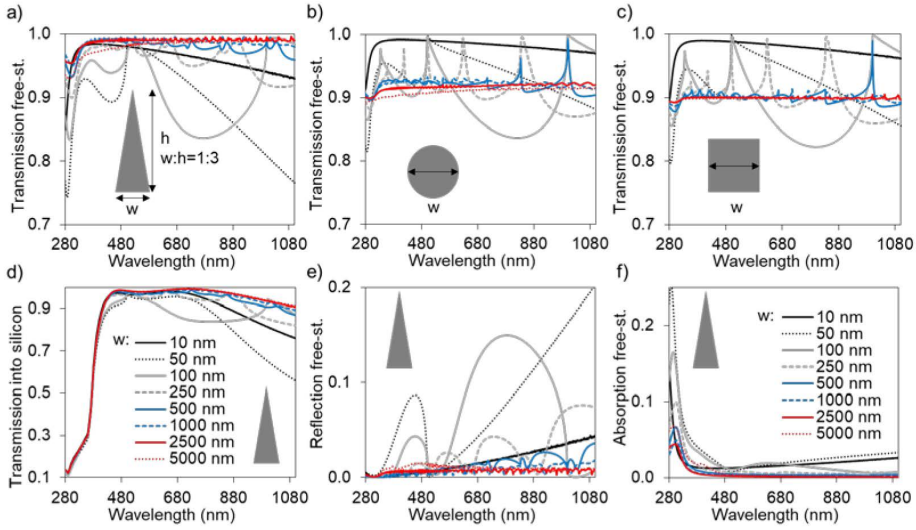

Fig. 2. Wavelength dependent transmission of free-standing a) triangle, b) circle and c) square cross-section silver structures with different width and 10% coverage. d) Transmission into silicon with triangle silver structures of different with and 10% coverage. e) Reflection and f) absorption within the silver of free-standing triangles.

We also performed RCWA simulations with the same metal structures but on top of a semiconductor with the optical properties of silicon [17]. We assumed a 50 nm TiO_2/100 nm SiO_2 antireflection coating on top of the silicon and infinite silicon thickness. We computed the transmission into the silicon, the reflection and the parasitic absorption of metal and antireflection coating. The transmission into silicon for triangles with 10% coverage is shown in Fig. 2(d). The transmission is reduced compared to free-standing triangles due to reflection at the silicon surface. Otherwise, the transmission features are comparable to the free-standing case. We performed the same simulations for all different configurations and weighted the results with the AM 1.5G solar spectrum in order to obtain a broad band average relevant for the case of solar cells. Figure 3 shows the weighted transmission for 3(a) circle, 3(b) triangle and 3(c) square cross-section silver structures with different coverage and different widths.

Optics EXPRESS

Circle and square structures outperform triangle cross-section in the nanoscale, but mesoscale triangles yield almost perfect transmission for all coverages. This is in accordance with publications of experimental results [7–9, 18–20]. Fig. 3(d)-3(f) show the calculated sheet resistance R_s of silver lines with different coverages, widths and shapes calculated by: $R_s = \rho L / A$ [18], where L is the pitch defined by the coverage and A the cross-section area. The specific resistance of silver ρ was assumed to be 1.6 μΩcm [21] and independent of the structure size. The sheet resistance decreases with increasing coverage, and also with increasing width as the height of the structures increases at the same time. Among these options, only mesoscale triangles achieve lower than 1 Ω/sq sheet resistance while also providing almost unity transmission. The contact resistance is usually assumed to scale with the inverse of the interface area [22] which corresponds to the coverage in our study. However, in nanoscale structures the contact barrier height can depend on the contact size [23] such that this simple correlation is no longer valid.

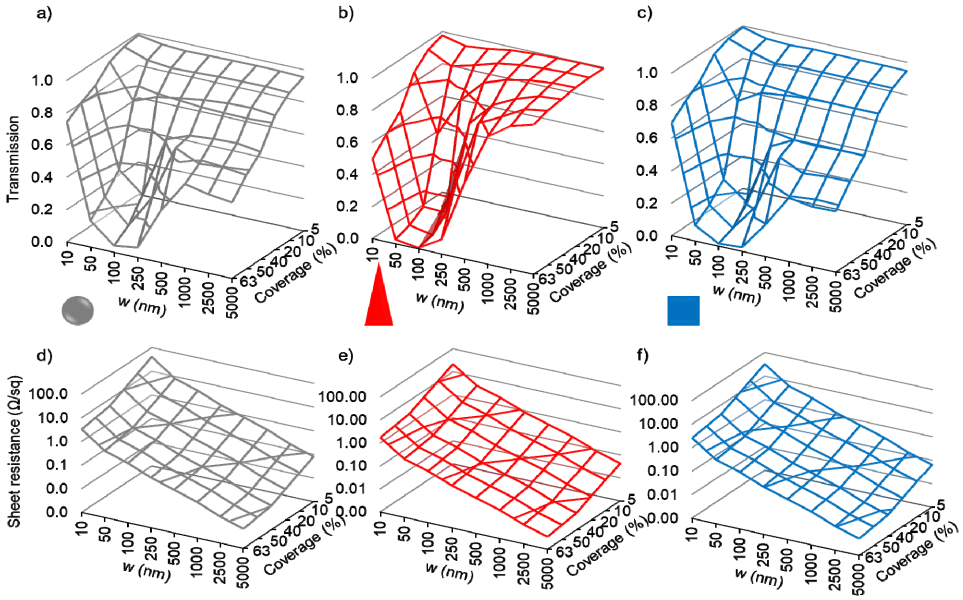

Fig. 3. Effective transparency weighted with the AM 1.5G solar spectrum depending on the width w and coverage of metallic structures on crystalline silicon with a) circle, b) triangle and c) square cross-section. Sheet resistance of silver lines with different width w, coverage and d) circle, e) triangle and f) square cross-section.

The results presented in Fig. 3 are consistent with previous studies that report on the transmission of silver nanogrids. As examples, T. Gao and P. W. Leu found a transmission of 90% and sheet resistance of 1.5 Ω/sq for a circle cross-section grid with width 90 nm and pitch 600 nm [12]. J.v.d.Groep et al. find 91% transmission and 6.5 Ω/sq for a square cross-section grid with 45 nm width and 1000 nm pitch [18]. If solar cells are encapsulated, the dielectric environment changes which has an influence on the contact transmission properties due to total internal reflection (TIR), coupling to surface plasmons and altered dipole emission. For nanoscale circular structures these effects were thoroughly investigated by Z. Zhao et al. who found for example that a 20 nm nanowire with 5% geometric coverage experiences only 4% shading [11]. Macroscopic circular shapes strongly benefit from TIR and in a typical encapsulation material such as EVA their actual shading is typically less than half of their geometric shading [24].

Optics EXPRESS

3. Light-trapping in silicon induced by densely spaced mesoscale silver grids

Mesoscale silver triangular contact arrays exhibit an additional particularly interesting property: The transmission of light depends on the angle of incidence [9]. Most obviously, while normally incident light is effectively transmitted as demonstrated above, light incident from the bottom reflects back toward the incidence direction from within the absorber. This effect can be used in order to create light trapping cavities in which the trapped light intensity can be enhanced compared to a dielectric absorber without contacts. We applied this property to the design of thin silicon solar cells to enhance absorption near the Si band edge via light trapping. Again, we performed RCWA simulations but this time we placed mesoscale silver triangular contact arrays (w = 2.5 µm, h = 7.0 µm) on top of 2 µm, 5 µm and 10 µm crystalline silicon absorber layers. We assumed a 50 nm TiO_2/100 nm SiO_2 antireflection coating on the top of the silicon and 100 nm SiO_2 with 300 nm silver as rear reflector. The wavelength dependent total absorption of the full structure with 2 µm crystalline silicon is shown in Fig. 4(a) for contact surface coverages of 0%, 4%, 50%, 63% and 83%. The inset shows a schematic of the simulated structure. We find that light absorption for wavelengths longer than 500 nm is lower than the transmission into the silicon indicated in Fig. 2(d). This is due to incomplete absorption in the thin silicon layers considered here, as silicon is an indirect semiconductor and therefore a weak absorber of low energy photons. As expected, 4% coverage follows the curve for 0% coverage, demonstrating ideal effective transparency. For higher coverage the absorption increases for short (300-400 nm) and long (>650 nm) wavelengths. Between 400 nm and 650 nm the absorption decreases with increasing coverage. Figure 4(b) shows the absorption within silicon and the absorption within the front metal triangular contacts. The absorption within the triangular contacts increases with increasing coverage and is most significant between 300 nm and 400 nm, which explains the increase in total absorption for this wavelength regime. For wavelengths >650 nm, absorption within the silicon increases with increasing contact surface coverage. Since silicon is an indirect semiconductor, not all the light close to the band edge is absorbed within one path through a 2 µm silicon layer. The cavity created by the array of closely spaced triangular contacts enhances the optical path length, and contributes to light trapping and enhanced absorption within the silicon. This is schematically depicted by the red arrow in the inset in Fig. 4(a).

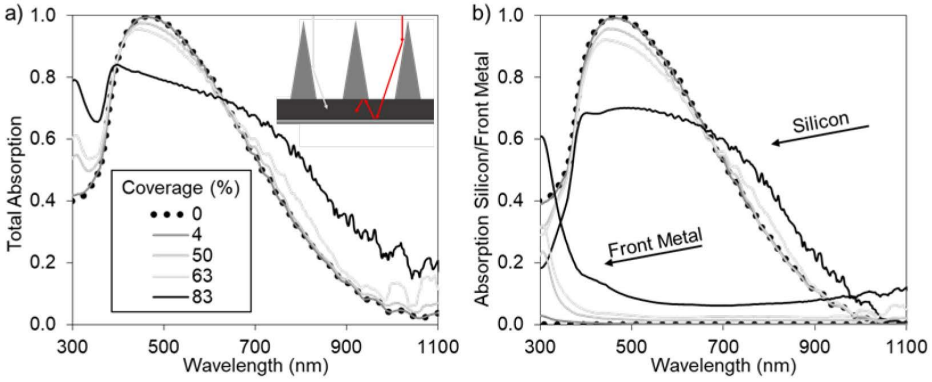

Fig. 4. Wavelength dependent a) Total absorption, b) Absorption within silicon and front metal absorption of 2 µm silicon with antireflection coating, rear reflector.and mesoscale triangular cross-section metallic grids on front. The inset in Fig. 4(a) shows a schematic of a 2 µm silicon absorber with mesoscale triangle contacts that enable effective transparence (grey arrow) and light trapping (red arrow).

We also assessed the absorption and transmission weighted by the AM 1.5G spectrum. In Fig. 5 we show the coverage-dependent total absorption and absorption within the silicon,

relative to a contact-free bare crystalline silicon absorber with 2 µm [Fig. 5(a)], 5 µm [Fig. 5(b)] and 10 µm [Fig. 5(c)] silicon thickness. The uncovered area fraction is marked by a black line with black circles. The absorption enhancement resulting from improved transmission into the silicon is shown by a black line with triangles and marked as grey area between the coverage and the transmission enhancement. The transmission was determined in a simulation with infinitely thick silicon in order to avoid superposition with escaped light. The red shaded area indicates the contribution to absorption from light trapping in the cavity consisting of a rear mirror and the front covered with triangular contact arrays, and the dark grey shaded area indicates the parasitic metal absorption generated by front and rear metal contact. In all three cases the total absorption surpasses the absorption without metal when covered with mesoscale silver triangular contact arrays with 63% surface coverage. At the same time, the absorption in the silicon is almost identical with the absorption without any metal. This surprising result is a superposition of the high effective transparency of mesoscale silver triangles in combination with the light trapping properties of densely spaced triangular contact arrays. We have shown previously [9] that the effective transparency of microscale triangular cross-section silver lines does not depend on the angle of incidence for light incident from an angle parallel to the contact line. Perpendicular to the contact line, the transmission experiences a cut-off at a specific angle that depends on the coverage.

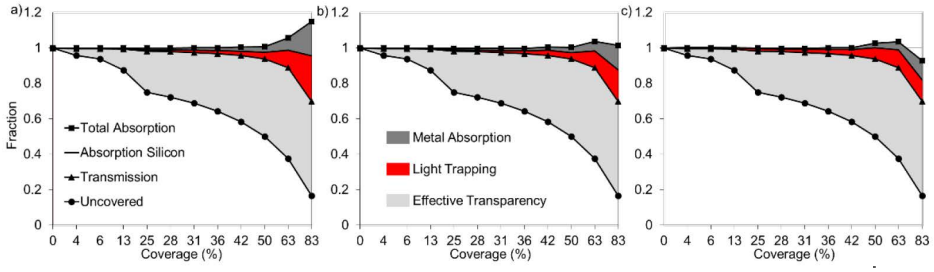

Fig. 5. Coverage dependent total absorption (black line with squares) and absorption within silicon (black line) with a) 2 µm, b) 5 µm and c) 10 µm thickness. The area fraction that is not covered by metal and the transmission into the silicon are shown by a black line with circles and triangles, respectively. The transmission was determined in a simulation with infinitely thick silicon in order to avoid superposition with escaped light. The area with increased absorption that is due to effective transparency is shown in light grey, light trapping is presented in red and parasitic absorption in front and rear metal are shown in dark grey. The total absorption and the absorption within silicon were calculated relative to a device with the same layer stack but without metal contacts (0% coverage).

Summary

We computationally investigated the absorption within silicon covered with silver contact arrays with different scales, shapes and coverages. Nanoscale contact structures with feature widths between 50 and 1000 nm experience parasitic resonant light absorption and reflection and therefore, are unfavorable for devices where high semiconductor absorption is required. We found that a 99% effective transparency and a 0.1 Ω/sq sheet resistance can be achieved simultaneously for mesoscale triangles with 20% coverage, 5µm width and 15 µm height. Furthermore, we found an absorption enhancement of up to 15% in 2 µm thick silicon absorber layers covered with densely spaced mesoscale triangular contact arrays. Our results show that for fundamental physics reasons, nanostructures cannot reach the transmission and the conductivity of triangular cross-section mesoscale silver contacts.

Funding

National Science Foundation (NSF) (EEC-1041895); Department of Energy (DOE) (EEC-1041895, DE-EE0004946); Global Climate & Energy project.

Optics EXPRESS

Acknowledgments

This material is based upon work supported by the Engineering Research Center Program of the National Science Foundation and the Office of Energy Efficiency and Renewable Energy of the Department of Energy under NSF Cooperative Agreement No. EEC-1041895 and by the U.S. Department of Energy through the Bay Area Photovoltaic Consortium under Award Number DE-EE0004946. RS acknowledges support from the Global Climate & Energy project.